RSC Advances

PAPER

View Article Online
View Journal | View Issue

Cite this: *RSC Adv.*, 2019, **9**, 307

A novel 3D Cd(II) coordination polymer generated *via in situ* ligand synthesis involving C–O ester bond formation†

Ji-Jiang Wang,* Zhuang Cao, Xiao Wang, Long Tang, Xiang-Yang Hou, Ping Ju, Yi-Xia Ren, Xiao-Li Chen and Yu-Qi Zhang

Received 19th July 2018
Accepted 10th December 2018

DOI: 10.1039/c8ra06112b

rsc.li/rsc-advances

A novel 3D Cd(II) coordination polymer $\{[Cd(ddpa)(2,2'\text{-bpy})]\cdot H_2O\}_n$ (1) (H_2ddpa = 5,10-dioxo-5,10-dihydro-4,9-dioxapyrene-2,7-dicarboxylic acid, 2,2′-bpy = 2,2′-bipyridine) is hydrothermally synthesized *in situ*, and the influencing factors and mechanism for the *in situ* reaction are briefly discussed. The synthesis of **1** requires the formation of a new C–O ester bond. This current study confirms that metal ions and N-donor ligands play important roles in the domination of the *in situ* ligand from 6,6′-dinitro-2,2′,4,4′-biphenyltetracarboxylic acid (H_4dbta). Furthermore, the structure, thermal stability and photoluminescent property of **1** are also investigated.

1. Introduction

Hydro(solvo)thermal *in situ* ligand syntheses are of great interest in coordination chemistry and organic chemistry for the preparation of unusual coordination compounds, discovery of new organic reactions and understanding their mechanisms.[1–5] So far, a variety of *in situ* ligand syntheses have already been reported, which include the formation of C–C, C–N, S–S, C–O, –O–, and C=C bonds,[6–11] oxidation of a phenyl ring with a methyl group,[12] formation of tetrazole,[13–15] and decarboxylation of aromatic carboxylates.[16] Since the hydro(solvo)thermal reaction is affected by several factors such as solvents, temperature, metal ions, organic ligands and anions,[17–24] it is still a formidable challenge to elucidate the reaction mechanism of *in situ* ligand syntheses.

It is well-known that the rational design and reasonable use of the organic multicarboxylate ligands are very important in the construction of desired coordination polymers. Although many studies have recently focused on the use of biphenyl-2,2′,4,4′-tetracarboxylic acid,[25–35] the use of 6,6′-dinitro-2,2′,4,4′-biphenyltetracarboxylic acid (H_4dbta) has not been adequately explored.[36–38] Compared with biphenyl-2,2′,4,4′-tetracarboxylic acid, although the nitro groups of H_4dbta might be unlikely to form coordination bonds with metal ions, they can influence the coordination and framework due to their electronegative and steric effects.[39]

Prior to this study, we reported the synthesis of a 3D pillared bilayer Cd(II) coordination polymer based on H_4dbta $\{[Cd_2(dbta)(dpe)]_n$, H_4dbta = 6,6′-dinitro-2,2′,4,4′-biphenyltetracarboxylic acid, dpe = 1,2-di(4-pyridyl)ethylene$\}$.[40] In a follow-up study, we found that the replacement of 1,2-di (4-pyridyl) ethylene (dpe) with 2,2′-bipyridine (2,2′-bpy) resulted in an *in situ* reaction containing a C–O ester bond in H_4dbta molecule to form the $ddpa^{2-}$ ligand ($ddpa^{2-}$ = 5,10-dioxo-5,10-dihydro-4,9-dioxapyrene-2,7-dicarboxylate; its ring system is identical to that of the natural tetracyclic diester ellagic acid), which resulted in the synthesis of another three-dimensional (3D) coordination polymer $\{[Cd(ddpa)(2,2'\text{-bpy})]\cdot H_2O\}_n$ (**1**). Although two coordination polymers of the $ddpa^{2-}$ ligand have been reported by Cheetham and Huang groups,[41,42] the synthesis of the $ddpa^{2-}$ ligand includes the *in situ* reaction of 5-hydroxyisophthalic acid (OH–H_2BDC) and Ni(II)/Ce(III) ions (Scheme 1). In this *in situ* synthesis, the formation of the C–O ester bond belongs to conventional esterifications, in which at least one –OH (hydroxyl) group of the carboxylic acids is replaced with an –O–alkyl (alkoxy) group. The most important difference between our work and the study reported by Cheetham and Huang groups is that we obtained the $ddpa^{2-}$ ligand by the *in situ* ligand synthesis of H_4dbta, Cd(II) and 2,2′-bpy (Scheme 2). Thus, it is necessary to explore the influencing factors for the *in situ* reaction of H_4dbta.

In this paper, the influencing factors and mechanism for the *in situ* generation of **1** are also briefly discussed. It is interesting that this *in situ* reaction is only observed when the metal ions and N-donor ligands are Cd(II) and 2,2′-bpy, respectively. If Cd(II) and 1,10-phenanthroline (phen)/dpe are used, 1D/3D structures of $\{[Cd_2(dbta)(phen)_2(H_2O)]\cdot H_2O\}_n$ (**2**) and $[Cd_2$

Yan'an University Key Laboratory of New Energy & New Function Materials, Shaanxi Key Laboratory of Chemical Reaction Engineering, College of Chemistry and Chemical Engineering, Yan'an University, Yan'an 716000, P. R. China. E-mail: yadxwjj@126.com

† Electronic supplementary information (ESI) available: Bond length/angle tables, figure of single-crystal, additional PXRD patterns, FT-IR, TGA. CCDC 1840510–1840512 for **1–3**. For ESI and crystallographic data in CIF or other electronic format see DOI: 10.1039/c8ra06112b

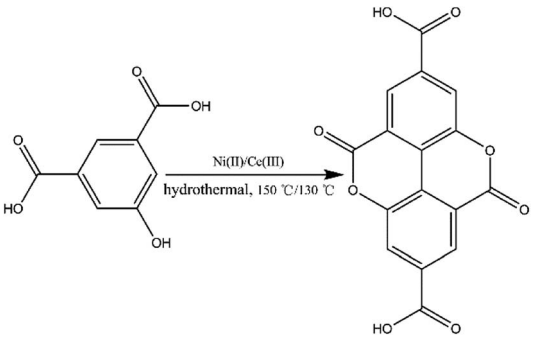

Scheme 1 *In situ* synthesis of the H_2ddpa ligand from OH–H_2bdc.

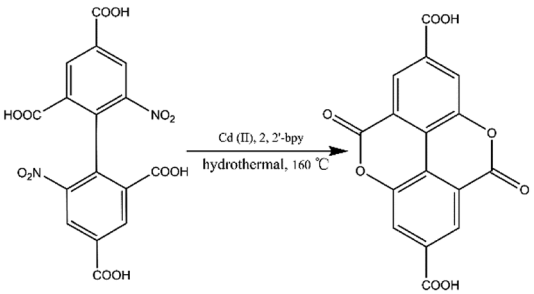

Scheme 2 *In situ* synthesis of the H_2ddpa ligand from H_4dbta.

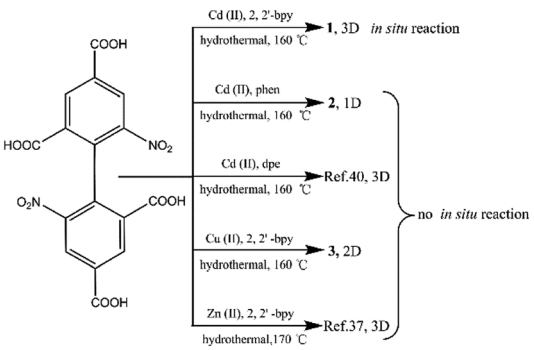

Scheme 3 The synthetic route for compounds **1–3**, $[Cd_2(dbta)(dpe)]_n$ (ref. 40) and $[Zn_2$ (dbta) (2,2′-bpy)$]_n$ (ref. 37).

(dbta) (dpe)$]_n$[40] are obtained by the hydrothermal reaction. In addition, the replacement of Cd(II) ions in **1** with Cu(II)/Zn(II) results in two different 2D/3D structures of $\{[Cu_2$ (dbta) (2,2′-bpy)$_2]\cdot H_2O\}_n$ (**3**) and $[Zn_2$ (dbta) (2,2′-bpy)$]_n$[37] (Scheme 3). As far as we know, this is the first example of a coordination polymer obtained *via in situ* synthesis of the H_4dbta ligand. Our study suggests that the synergetic effects of both 2,2′-bpy and Cd(II) ions are important factors in controlling the formation of the ddpa^{2-} ligand. In this *in situ* synthesis, the formation of the C–O ester bond was not by conventional esterifications, which expands the conception of esterifications in organic chemistry. The result provides a promising route to design and construct a new organic ligand with special structures and properties. Furthermore, the thermal stability and photoluminescent properties of **1–3** are also investigated.

2. Experimental

2.1 Materials and methods

All reagents and solvents employed were commercially available and used without further purification. The C, H and N microanalyses were carried out with a PE 2400 Series II elemental analyzer. The IR spectra were recorded with a Shimadzu IR Affinity-1 spectrometer using the KBr pellet technique. Thermogravimetric analysis was performed on a NETZSCH STA 449F3 analyzer. The powder X-ray diffraction (PXRD) measurement was carried out using a Shimadzu XRD-7000 diffractometer with Cu Kα radiation (λ = 1.5418 Å). Photoluminescence spectra were obtained on a Hitachi F-4500 fluorescence spectrophotometer at room temperature.

2.2 Synthetic procedures

2.2.1 Synthesis of $\{[Cd$ (ddpa) (2,2′-bpy)$]\cdot H_2O\}_n$ (1). A mixture of CdO (0.0064 g, 0.05 mmol), H_4dbta (0.0210 g, 0.05 mmol), 2,2′-bpy (0.0078 g, 0.05 mmol) and 10 mL H_2O was stirred for 30 min. The mixture was then placed in a 25 mL Teflon-lined stainless steel vessel and heated at 160 °C for 3 d. Yellow block crystals were obtained when the mixture was cooled to room temperature. Yield: *ca.* 56% based on Cd. Calcd. for $C_{26}H_{14}CdN_2O_9$ (%): C, 51.13; H, 2.31; N, 4.59. Found (%): C, 50.42; H, 2.38; N, 4.69. IR (KBr pellet, cm^{-1}): 3488 m, 1743 s, 1625 m, 1593 m, 1549 s, 1372 s, 1294 s, 1186 s, 1091 s, 1014 m, 805 m, 766 m, 696 m, 652 w, 576 w, 525 w.

2.2.2 Synthesis of $\{[Cd_2$ (dbta) (phen)$_2$ (H_2O)$]\cdot H_2O\}_n$ (2). The preparation of **2** was similar to that of **1** except that phen (0.0099 g, 0.05 mmol) was used instead of 2,2′-bpy (0.0078 g, 0.05 mmol). Yellow block crystals were obtained. Yield: *ca.* 62% based on Cd. Calcd. for $C_{40}H_{24}Cd_2N_6O_{14}$ (%): C, 46.31; H, 2.33; N, 8.10. Found (%): C, 45.59; H, 2.35; N, 8.21. IR (KBr pellet, cm^{-1}): 3488 w, 3068 w, 2362 w, 1599 w, 1561 w, 1523 m, 1434 m, 1389 m, 1338 s, 1097 w, 932 m, 925 w, 843 s, 728 s, 785 m, 716 s, 626 w, 544 w, 423 w.

2.2.3 Synthesis of $\{[Cu_2$ (dbta) (2,2′-bpy)$_2]\cdot H_2O\}_n$ (3). The preparation of **3** was similar to that of **1** except that CuO (0.0080 g, 0.1 mmol) was used instead of CdO (0.0064 g, 0.05 mmol). Blue plate block crystals were obtained. Yield: *ca.* 45% based on Cu. Calcd. for $C_{36}H_{22}Cu_2N_6O_{13}$ (%): C, 49.49; H, 2.54; N, 9.62. Found (%): C, 49.71; H, 2.42; N, 9.21. IR (KBr pellet, cm^{-1}): 3434 m, 1620 s, 1593 m, 1536 s, 1441 m, 1390 m, 1328 s, 1098 w, 761 m, 717 m, 627 w, 515 w, 414 w.

2.3 X-ray data collection and structure determination

Intensity data were collected on a Bruker Smart APEX II CCD diffractometer equipped with graphite-monochromated Mo-Kα radiation (λ = 0.71073 Å) using ω–φ scan mode. A semi-empirical absorption correction was applied using the SADABS program.[43] The structure was solved with direct methods and refined by full-matrix least-squares on F^2 using the SHELXS-2014/7 and SHELXL-2014/7 programs, respectively.[44,45] Non-hydrogen atoms were refined anisotropically and hydrogen atoms were placed in the geometrically calculated positions. The (dbta)$^{4-}$ anions and lattice water molecules in 3 were

disordered and refined with different occupancy ratios. The hydrogen atoms of the disordered lattice water molecules in 3 were not added. The crystallographic data and selected bonds and angles for **1–3** are given in Tables S1 and S2,† respectively.

3. Results and discussion

3.1 Syntheses and characterization

The hydrothermal reactions of CdO and 6,6′-dinitro-2,2′,4,4′-biphenyltetracarboxylic acid (H_4dbta) with 2,2′-bpy gave the 3D framework of **1**. To explore the influencing factors and formation mechanism for the *in situ* reaction of H_4dbta in **1**, compounds **2** and **3** were synthesized under hydrothermal conditions (Scheme 3). When N-donor phen/dpe ligands were used instead of 2,2′-bpy in **1**, a structurally different 1D chain/3D pillared bilayer framework was formed in **2** and $[Cd_2(dbta)(dpe)]_n$[40] under similar reaction conditions. Similarly, the replacement of Cd(II) ions in **1** by Cu(II)/Zn(II) resulted in two different 2D network/3D "brick-wall" frameworks.[37] Apparently, the *in situ* reaction of H_4dbta to H_2ddpa did not occur for compounds **2** and **3**, which suggests that the metal ions and N-donor ligands have great effect on the *in situ* reaction.

For compounds **1–3**, the elemental analyses were consistent with their chemical formulae. PXRD showed that the observed patterns for **1** and **2** correlate well with the simulated patterns generated from the single-crystal X-ray diffraction data (Fig. S2 and S3,†). In the IR spectra of **1–3** (Fig. S4,†), the absence of any strong bands around 1700 cm^{-1} indicates that all the carboxylic groups are depronated. For **1**, a sharp absorption band at 1743 cm^{-1} is observed, confirming the existence of the $\nu_{C=O}$ group. The absorption bands at 1372 and 1186 cm^{-1} for **1** can be assigned to the vibrations of ν^{as}_{C-O-C} and ν^{s}_{C-O-C} groups, respectively. Thermal stability studies (Fig. S5,†) demonstrate that **1** is thermally stable up to 250 °C; then, a quick weight loss (*ca.* 55%) from 250 to 360 °C is observed, which is caused by the decomposition of ligands. For **2**, weight loss of about 3.6% is observed from 25 to 166 °C, which is ascribed to the release of lattice and coordinated water, followed by a quick weight loss of about 65.6% from 285 to 373 °C. For **3**, weight loss of about 2.2% is observed from 25 to 117 °C, which may be ascribed to the release of lattice water; this is followed a quick weight loss of about 47.8% from 225 to 276 °C. The second step of the weight loss for **2** and **3** is caused by the decomposition of the ligands.

3.2 Structural descriptions

3.2.1 {[Cd (ddpa) (2,2′-bpy)] ·H_2O}$_n$ (1). The X-ray analysis reveals that **1** crystallizes in the space group *C*2/*c* and has a 3D framework containing a 1D inorganic chain (–Cd–O–C–O–Cd–). As shown in Fig. 1a, each asymmetric unit of **1** contains one Cd(II) ion, one $ddpa^{2-}$ ligand, one 2,2′-bpy ligand and one lattice H_2O molecule. The Cd(II) ion is coordinated by four oxygen atoms from four different $ddpa^{2-}$ ligands and two nitrogen atoms from one 2,2′-bpy ligand to furnish distorted octahedral coordination geometry. All the Cd–O and Cd–N bond lengths are in accordance with those reported in other related ref. 46 and 47 The two carboxyl groups in each $ddpa^{2-}$ ligand adopt

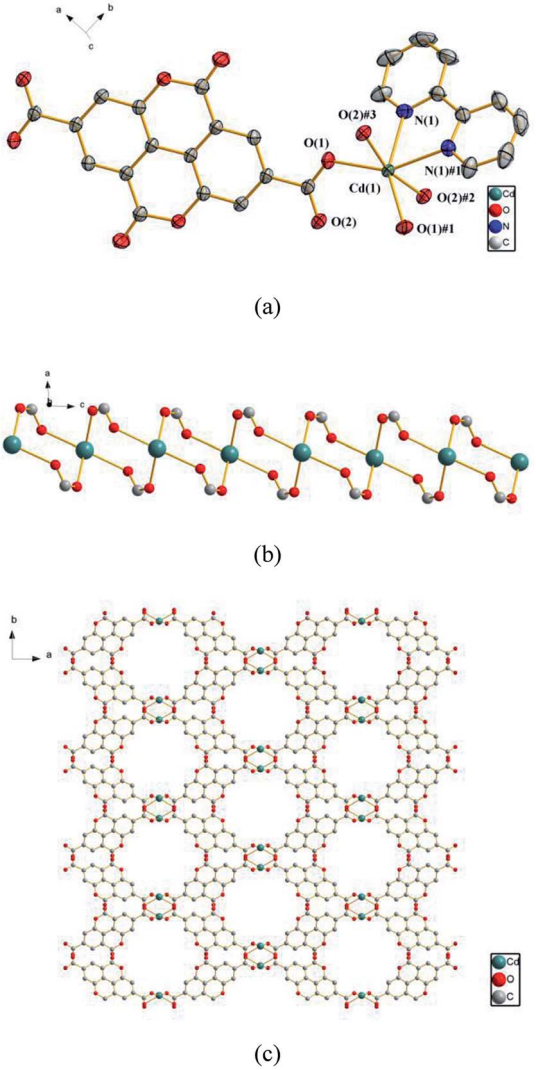

Fig. 1 (a) The coordination environments of Cd(II) ions in **1**, symmetry codes: #1: $-x, y, -z + 1/2$; #2: $-x, -y, -z + 1$; #3: $x, -y, z - 1/2$. All hydrogen atoms are omitted for clarity. (b) The 1D chain (–Cd–O–C–O–Cd–) in **1**. (c) The 3D framework assembled from the 1D chains. The 2,2′-bpy molecules, lattice water and hydrogen atoms are omitted for clarity.

a μ^2-η^1:η^1 coordination mode to connect the adjacent Cd(II) ions and generate a 1D inorganic chain (–Cd–O–C–O–Cd–) (Fig. 1b). In the 1D chains formed by dinuclear rings, the Cd(II)···Cd(II) distance is 4.3658(2) Å. Along the *c* axis, such a chain is further linked by $ddpa^{2-}$ ligands to generate a 3D framework structure (Fig. 1c). The whole framework has octagonal-prism-like 1D channels filled with 2, 2′-bpy ligands and lattice H_2O molecules, and the effective solvent accessible volume is 147 $Å^3$ per unit cell (6.4% of the total cell volume calculated by the Platon program).

3.2.2 {[Cd_2 (dbta) (phen)$_2$ (H_2O)]·H_2O}$_n$ (2). To further examine the influence of the N-donor ligands on the structure of **1**, a larger sized aromatic chelate ligand phen is used instead of 2,2′-bpy. Consequently, compound **2**, which features a 1D looped chain, is obtained. Compound **2** crystallizes in the triclinic space group $P\bar{1}$. In the asymmetric unit, there exist two crystallographically unique Cd(II) ions, one $dbta^{4-}$ ligand, two

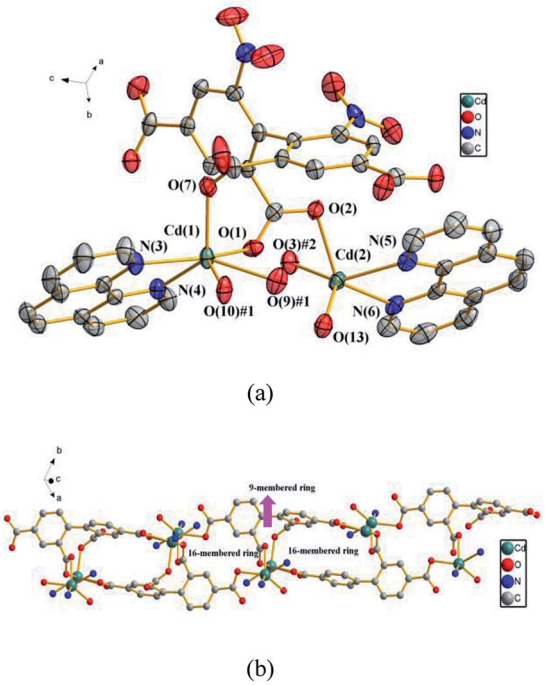

Fig. 2 (a) The coordination environments of Cd(II) ions in **2**, symmetry codes: #1: $-x, y, -z + 1/2$; #2: $-x, -y, -z + 1$; #3: $x, -y, z - 1/2$. All hydrogen atoms are omitted for clarity. (b) The 1D looped chain in **2**. The phen ligands, nitro groups and hydrogen atoms are omitted for clarity.

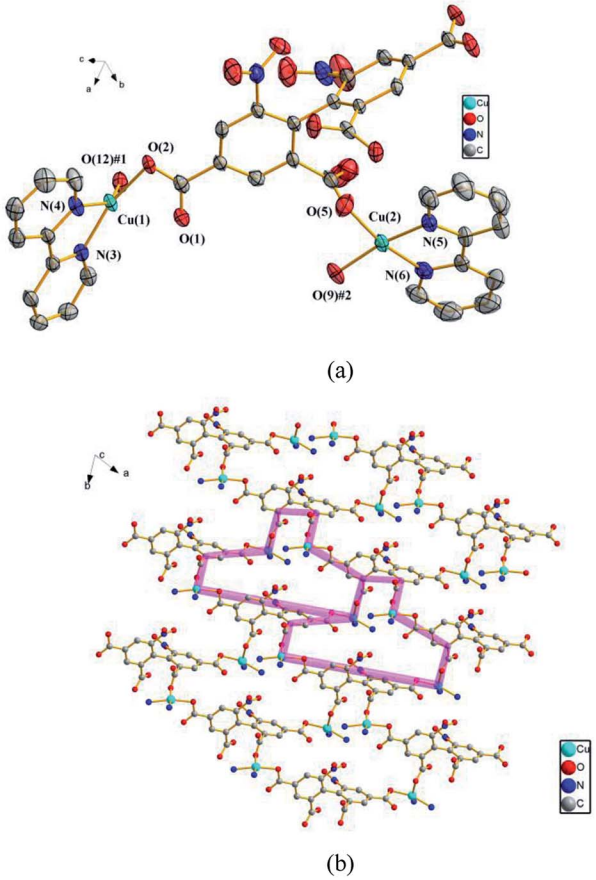

Fig. 3 (a) The coordination environments of Cu(II) ions in **3**, symmetry codes: #1: $-x, y, -z + 1/2$; #2: $-x, -y, -z + 1$; #3: $x, -y, z - 1/2$. All hydrogen atoms are omitted for clarity. (b) The 2D convex-shaped network in **2**. The 2,2′-bpy molecules and hydrogen atoms are omitted for clarity.

phen ligands, one coordinated H_2O molecule and one lattice H_2O. As illustrated in Fig. 2a, the Cd (**1**) ion exhibits distorted octahedral geometry and is coordinated by two nitrogen atoms from a chelate phen and four oxygen atoms from three carboxylic groups of two $dbta^{4-}$ ligands. The Cd (**2**) ion is ligated by two nitrogen atoms from a chelate phen, one oxygen atom from one coordinated H_2O molecule and two oxygen atoms from two $dbta^{4-}$ ligands to form distorted tetragonal pyramid geometry. These bond lengths are similar to those found in related dicadmium-tetracarboxylate polymers.[37] The four carboxylate groups of the $dbta^{4-}$ ligands adopt three different coordination modes, *i.e.*, monodentate, chelating bidentate and bridging bidentate to generate a 1D looped chain containing a 16-membered ring and a 9-membered ring (Fig. 2b).

3.2.3 $\{[Cu_2(dbta)(2,2'\text{-bpy})_2]\cdot H_2O\}_n$ (3). To further explore the influence of metal ions on the structure of **1**, Cu(II) ion is used instead of Cd(II) ion. Consequently, compound **3**, which features a 2D network, is obtained. Compound **3** crystallizes in the triclinic space group $P\bar{1}$. In the asymmetric unit, there exist two crystallographically unique Cu(II) ions, one $dbta^{4-}$ ligand, two 2,2′-bpy ligands and one free H_2O molecule. As illustrated in Fig. 3a, Cu (**1**) and Cu (**2**) ions exhibit distorted square geometry and are coordinated by two nitrogen atoms from a chelate 2,2′-bpy and two oxygen atoms from two carboxylic groups of two $dbta^{4-}$ ligands. The four carboxylate groups of $dbta^{4-}$ ligands adopt monodentate coordination modes. Each Cu(II) ion is bridged by $dbta^{4-}$ ligands to form a 2D convex-shaped network extending along the *ab* plane (Fig. 3b).

3.3 Influencing factors and mechanism for the *in situ* generation of $ddpa^{2-}$

To evaluate whether both 2,2′-bpy and Cd(II) ions play crucial roles in the reaction process, after replacing 2,2′-bpy by phen/dpe ligands, the 1D looped chain/3D pillared bilayer framework was formed in **2** and $[Cd_2(dbta)(dpe)]_n$[40] under similar reaction conditions, respectively. Compound **2** and $[Cd_2(dbta)(dpe)]_n$ contain no $ddpa^{2-}$ ligand, suggesting that the *in situ* reaction may be prohibited. To further explore this interesting phenomenon, Cu(II) ion/Zn(II) is used instead of Cd(II) ion, followed by the same procedure as that for **1**. The 2D network of **3** and the 3D "brick-wall" framework[37] were obtained as new phases, indicating that Cu(II)/Zn(II) anions have the same negative effect on the *in situ* reaction as phen/dpe. Therefore, it can be concluded that the *in situ* reaction of the $dbta^{4-}$ ligand resulted from synergetic effects of both 2,2′-bpy and Cd(II) ions under hydrothermal conditions. This phenomenon is greatly different from the *in situ* generation of $ddpa^{2-}$ within the Ni(II)/Ce(III) reaction system.[41,42]

The possible mechanism for the *in situ* generation of $ddpa^{2-}$ was postulated and displayed in Scheme 4. An intramolecular nucleophilic aromatic substitution reaction (SNAr) may have

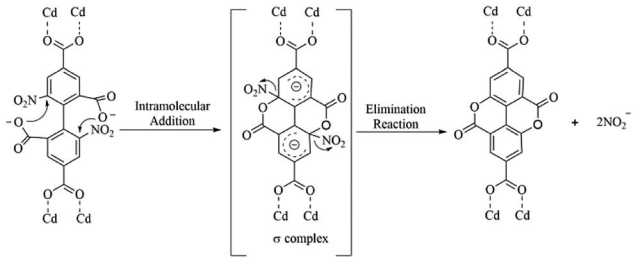

Scheme 4 The possible mechanism for *in situ* generation of $ddpa^{2-}$.

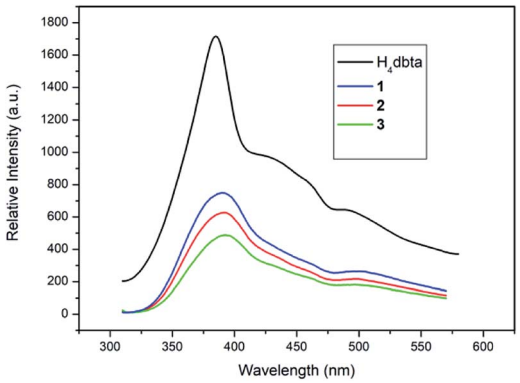

Fig. 4 The emission spectra of free H_4dbta and **1–3** in the solid state at room temperature.

occurred during hydrothermal synthesis processes. As shown in Scheme 4, the protonated carboxyl groups serve as nucleophilic agents to form the σ-complex intermediate (addition reaction), which can generate the cyclization products by eliminating the nitroso-group (elimination reaction). To illustrate the above plausible mechanism, several drops of $AgNO_3$ solution (0.1 mol L^{-1}) were added into the filtrate of the reaction mixture, and a large faint yellow precipitate was formed immediately, which revealed that $AgNO_2$ might be formed. The clarification of the mechanism for internal esterifications as well as the origin of the synergy between 2, 2′-bpy and Cd(II) ion under hydrothermal conditions requires further studies, which are currently underway in our laboratory.

3.4 Photoluminescent properties

The solid state luminescence of free H_4dbta and **1–3** was investigated at room temperature (Fig. 4). Upon excitation at 296 nm, the free H_4dbta exhibits intense emission at 384 nm. Compounds **1–3** exhibited photoluminescence with emission maxima at 390 nm (**1** and **2**) and 393 nm (**3**), respectively. The three compounds exhibit a red-shift compared with the free H_4dbta ligand. Compounds **1–3** exhibit similar emission peaks to the free H_4dbta ligand. We tentatively assign them to intra-ligand photoluminescence.[48,49] The different red-shifts and intensities of the emission of three compounds compared to that of the free H_4dbta ligand may result from the differences in the coordination environments and different structures and *in situ* ligands.

4. Conclusions

In summary, a novel 3D Cd(II) coordination polymer is hydrothermally synthesized *in situ*, and the influencing factors and mechanism for the *in situ* reaction are briefly discussed. The formation of **1** suggests that the *in situ* reaction for the $dbta^{4-}$ ligand resulted from synergetic effects of both 2,2′-bpy and Cd(II) ion under hydrothermal conditions. A study of the mechanism indicates that an intramolecular nucleophilic aromatic substitution reaction (SNAr) may have occurred during hydrothermal synthesis processes. The study also reveals that C–O ester bonds can also be formed *in situ* by H_4dbta, which provides a promising route to design and construct a new organic ligand with special structures and properties. In the future, we will further clarify the mechanism for the internal esterifications as well as the origin of the synergy between 2,2′-bpy and Cd(II) ions under hydrothermal conditions.

Conflicts of interest

There are no conflicts to declare.

Acknowledgements

This work was financially supported by the NSF of China (No. 21373178, 21663031 and 21503183), which are gratefully acknowledged.

References

1 X. M. Zhang, *Coord. Chem. Rev.*, 2005, **249**, 1201–1219.
2 X. M. Chen and M. L. Tong, *Acc. Chem. Res.*, 2007, **40**, 162–170.
3 Y. C. Chang and S. L. Wang, *J. Am. Chem. Soc.*, 2012, **134**, 9848–9851.
4 E. T. Nguyen, X. Zhao, D. Ta, P. L. Nguyen and X. H. Bu, *Cryst. Growth Des.*, 2015, **15**, 5939–5944.
5 T. Huang, Y. L. Wang, Q. Yin, B. Karadeniz, H. F. Li, J. Lü and R. Cao, *CrystEngComm*, 2016, **18**, 2742–2747.
6 G. B. Li, J. M. Liu, Z. Q. Yu, W. Wang and C. Y. Su, *Inorg. Chem.*, 2009, **48**, 8659–8661.
7 A. K. Ghosh, T. S. Mahapatra, R. Clérac, C. Mathonière, V. Bertolasi and D. Ray, *Inorg. Chem.*, 2015, **54**, 5136–5138.
8 C. E. Rowland, N. Belai, K. E. Knope and C. L. Cahill, *Cryst. Growth Des.*, 2010, **15**, 1390–1398.
9 P. Kanoo, R. Matsuda, H. Sato, L. C. Li, H. J. Jeon and S. Kitagawa, *Inorg. Chem.*, 2013, **52**, 10735–10737.
10 X. M. Zhang, J. J. Hou and H. S. Wu, *Dalton Trans.*, 2004, 3437–3439.
11 F. L. Yang, J. Tao, R. B. Huang and L. S. Zheng, *Inorg. Chem.*, 2011, **50**, 911–917.
12 D. Wu, X. J. Bai, H. R. Tian, W. T. Yang, Z. W. Li, Q. Huang, S. Y. Du and Z. M. Sun, *Inorg. Chem.*, 2015, **54**, 8617–8624.
13 L. Sun, L. Ma, J. B. Cai, L. Liang and H. Deng, *CrystEngComm*, 2012, **14**, 890–898.

14 R. T. Dong, Z. Y. Ma, L. X. Chen, L. F. Huang, Q. H. Li, M. Y. Hu, M. Y. Shen, C. W. Li and H. Deng, *CrystEngComm*, 2015, **17**, 5814–5831.
15 C. C. Chang, Y. C. Huang, S. M. Huang, J. Y. Wu, Y. H. Liu and K. L. Lu, *Cryst. Growth Des.*, 2012, **12**, 3825–3828.
16 M. A. Nadeem, M. Bhadbhade, R. Bircher and J. A. Stride, *Cryst. Growth Des.*, 2010, **10**, 4060–4067.
17 W. Q. Zhang, W. Y. Zhang, R. D. Wang, C. Y. Ren, Q. Q. Li, Y. P. Fan, B. Liu, P. Liu and Y. Y. Wang, *Cryst. Growth Des.*, 2017, **17**, 517–526.
18 B. Liu, L. Wei, N. N. Li, W. P. Wu, H. Miao, Y. Y. Wang and Q. Z. Shi, *Cryst. Growth Des.*, 2014, **14**, 1110–1127.
19 Y. P. He, L. B. Yuan, H. Xu and J. Zhang, *Cryst. Growth Des.*, 2017, **17**, 290–294.
20 H. Wang, G. J. Xing, F. Chen, J. Sun and Y. H. Zhang, *Chin. J. Struct. Chem.*, 2015, **34**, 1113–1120.
21 L. Qin, J. S. Hu, Y. Z. Li and H. G. Zheng, *Cryst. Growth Des.*, 2012, **12**, 403–413.
22 J. J. Liu, Y. F. Guan, M. J. Lin, C. C. Huang and W. X. Dai, *Cryst. Growth Des.*, 2016, **16**, 2836–2842.
23 E. Lee, H. Ju, S. Kim, K. M. Park and S. S Lee, *Cryst. Growth Des.*, 2015, **15**, 5427–5436.
24 B. Hu, T. Tao, Z. Y. Bin, Y. X. Peng, B. B. Ma and W. Huang, *Cryst. Growth Des.*, 2014, **14**, 300–309.
25 T. T. Jia, S. R. Zhu, M. Shao, Y. M. Zhao and M. X. Li, *Inorg. Chem. Commun.*, 2008, **11**, 1221–1223.
26 L. L. Wen, F. Wang, X. K. Leng, C. G. Wang, L. Y. Wang, J. M. Gong and D. F. Li, *Cryst. Growth Des.*, 2010, **10**, 2835–2838.
27 L. Cheng, S. H. Gou and J. Q. Wang, *J. Mol. Struct.*, 2011, **991**, 149–157.
28 J. J. Wang, T. T. Wang, L. Tang, X. Y. Hou, L. J. Gao, F. Fu and M. L. Zhang, *J. Coord. Chem.*, 2013, **66**, 3979–3988.
29 J. Jia, M. Shao, T. T. Jia, S. R. Zhu, Y. M. Zhao, F. F. Xing and M. X. Li, *CrystEngComm*, 2010, **12**, 1548–1561.
30 W. X. Chen, H. R. Xu, G. L. Zhuang, L. S. Long, R. B. Huang and L. S. Zheng, *Chem. Commun.*, 2011, **47**, 11933–11935.
31 Y. H. Su, F. Luo, H. Li, Y. X. Che and J. M. Zheng, *CrystEngComm*, 2011, **13**, 44–46.
32 Z. R. Pan, J. Xu, Xi. Q. Yao, Y. Z. Li, Z. J. Guo and H. G. Zheng, *CrystEngComm*, 2011, **13**, 1617–1624.
33 H. Tian, K. Wang, Q. X. Jia, Q. Sun, Y. Ma and E. Q. Gao, *Cryst. Growth Des.*, 2011, **11**, 5167–5170.
34 F. Su, L. P. Lu and S. S. Feng, *J. Mol.Struct.*, 2015, **1096**, 38–42.
35 F. Su, L. P. Lu, S. S. Feng, M. L. Zhu, Z. Q. Gao and Y. H. Dong, *Dalton Trans.*, 2015, **44**, 7213–7222.
36 C. Y. Ren, B. Liu, W. P. Wu, P. Liu, G. P. Yang, Y. F. Kang and Y. Y. Wang, *Inorg. Chem. Commun.*, 2015, **53**, 46–49.
37 Q. Q. Li, W. Q. Zhang, C. Y. Ren, Y. P. Fan, J. L. Li, P. Liu and Y. Y. Wang, *CrystEngComm*, 2016, **18**, 3358–3371.
38 W. Q. Zhang, W. Y. Zhang, R. D. Wang, C. Y. Ren, Q. Q. Li, Y. P. Fan, B. Liu, P. Liu and Y. Y. Wang, *Cryst. Growth Des.*, 2017, **17**, 517–526.
39 J. Y. Zhang, X. H. Jing, Y. Ma, A. L. Cheng and E. Q. Gao, *Cryst. Growth Des.*, 2011, **11**, 3681–3685.
40 J. W. Wang, Y. C. Su and J. J. Wang, *Chin. J. Struct. Chem.*, 2015, **34**, 1385–1390.
41 R. K. Feller, P. M. Forster, F. Wudl and A. K. Cheetham, *Inorg. Chem.*, 2007, **46**, 8717–8721.
42 X. Y. Cao, L. Q. Yu and R. D. Huang, *J. Solid State Chem.*, 2014, **210**, 74–78.
43 G. M. Sheldrick, *SADABS, A Program for Empirical Absorption Correction of Area detector Data*, University of Göttingen, Germany 1997.
44 G. M. Sheldrick, *SHELXS-2014/7, Program for Crystal Structure Solution*, University of Göttingen, Germany 2014.
45 G. M. Sheldrick, *SHELXL-2014/7, Program for Crystal Structure Refinement*, University of Göttingen, Germany 2014.
46 J. J. Wang, M. L. Yang, H. M. Hua, G. L. Xue, D. S. Li and Q. Z. Shi, *Z. Anorg. Allg. Chem.*, 2007, **633**, 341–345.
47 L. L. Liu, C. X. Yu, Y. R. Li, J. J. Han, F. J. Ma and L. F. Ma, *CrystEngComm*, 2015, **17**, 653–664.
48 C. C. Du, X. F. Wang, S. B. Zhou, D. Z. Wang and D. Z. Jia, *CrystEngComm*, 2017, **19**, 6758–6777.
49 D. Chisca, L. Croitor, O. Petuhov, O. V. Kulikova, G. F. Volodina, E. B. Coropceanu, A. E. Masunov and M. S. Fonari, *CrystEngComm*, 2018, **20**, 432–447.